Chemical Science

RSC Publishing

EDGE ARTICLE

View Article Online
View Journal | View Issue

Expanding DNAzyme functionality through enzyme cascades with applications in single nucleotide repair and tunable DNA-directed assembly of nanomaterials†

Cite this: *Chem. Sci.*, 2013, 4, 398

Yu Xiang,[a] Zidong Wang,[b] Hang Xing[a] and Yi Lu*[ab]

Many biological functions require two or more enzymes working together in cascades. While many examples of protein and RNA enzyme cascades are known, few enzyme cascades containing solely DNAzymes have been reported. Herein we demonstrate the combination of an 8–17 DNAzyme with RNA cleavage activity and an E47 DNAzyme with DNA ligation activity to achieve a new function of single ribonucleotide repair in DNA while maintaining the integrity of the original DNA sequence, which is difficult for a single DNAzyme to achieve. In addition, this method is applied to modify the sequences of DNA strands immobilized on the surface of nanoparticles to control the DNA-directed assembly selectively and sequentially. Such an approach can be applied to other DNAzymes with different activities to expand the functions of DNAzymes and the scope of their applications.

Received 15th June 2012
Accepted 19th September 2012

DOI: 10.1039/c2sc20763j

www.rsc.org/chemicalscience

Introduction

The discovery of deoxyribozymes (DNAzymes) with enzymatic activity in the 1990s[1,2] has demonstrated that DNA molecules are not simply inert biopolymers for genetic storage; they can be active catalysts as well.[3–8] Since then, many DNAzymes have been obtained with catalytic functions such as cleavage,[2,9–13] ligation,[14–16] phosphorylation,[17] adenylation[18] or depurination[19] of nucleic acids, as well as other reactions including porphyrin metallation, C–C bond formation, nucleopeptide linkage formation, oxygen transfer and thymine dimer repair.[20–26] Because DNAzymes are facile to synthesize and more stable than protein and RNA enzymes, they have been widely used in applications such as nanomaterial assembly,[27,28] biosensing,[29–31] logical computing,[32] nanomachine engineering,[33] antiviral or gene therapy,[34] and *in vitro* RNA manipulation.[35] Despite these successes, the application of DNAzymes is limited by the narrower range of catalytic functionality compared to protein enzymes. One possible approach to addressing this issue would be to combine enzymes with different reactivities to form a cascade of successive enzymatic reactions, which together create new functionality. Indeed, many such examples exist in biology, since nearly all important biological functions, such as the pathways involved in DNA repair and protein synthesis, require a cascade of multiple protein enzymes to carry out their full function. In contrast, little has been reported about the use of DNAzyme cascades to realize enhanced functionality. Such a strategy could expand the functionality of DNAzymes to a level more on par with protein and RNA enzymes, which should greatly increase the range of possible applications.

One such application is single nucleotide repair, *i.e.*, excision of a misincorporated ribonucleotide in single-stranded DNA and subsequent insertion of the corresponding deoxyribonucleotide at the excision site. The misincorporation of ribonucleotides into DNA strands can occur from exposure to external oxidizing agents or ionizing radiation,[36] or spontaneously during DNA replication.[37] Misincorporation of ribonucleotide can distort the structure of DNA,[38] reduce its stability,[39] and interfere with the normal interaction between DNA and DNA polymerases.[40] In fact, the overexpression of DNA polymerases that are prone to ribonucleotide misincorporation has been linked to many cancers, including ovarian, prostate, breast and colon cancers.[41] In nature, protein enzymes such as RNase H and FEN-1 can efficiently excise misincorporated ribonucleotides in DNA by cleaving the DNA at the ribonucleotide site and then restoring the correct deoxyribonucleotides by DNA polymerases,[42,43] which is an example of an enzyme cascade. It would be interesting to find out if a similar function could be achieved through DNAzyme cascades.

Another potential application is in tuning the properties of DNA-functionalized nanomaterials. For example, DNA-functionalized gold nanoparticles[27] have emerged as an attractive platform for biosensing,[32,44–50] nanomedicine,[45] and as building blocks for controlled nanoassemblies.[51–55] Although much research has been focused on the surface modification of gold nanoparticles with DNA for various applications, there are still

[a]*Department of Chemistry, University of Illinois at Urbana-Champaign, Urbana, IL 61801, USA*

[b]*Department of Material Science, University of Illinois at Urbana-Champaign, Urbana, IL 61801, USA. E-mail: yi-lu@illinois.edu; Fax: +1 217-244-3186; Tel: +1 217-333-2619*

† Electronic supplementary information (ESI) available. See DOI: 10.1039/c2sc20763j

limited methods to modify the sequences of DNA already immobilized on gold nanoparticles in order to make the properties of the DNA-modified nanomaterials tunable after fabrication. The use of DNAzymes is a promising approach for DNA modification on nanomaterials[56] due to the excellent stability of DNAzymes and their smaller size compared to protein enzymes, thereby minimizing steric effects between the enzyme and the DNA in order to avoid reduction in reaction efficiency. However, it is still very challenging to modify a specific DNA sequence on multiple-DNA-functionalized nanomaterials to tune their functions in a selective and sequential fashion.

Herein, we demonstrate a cascade of two DNAzymes with RNA cleavage and DNA ligation activities, respectively, in order to carry out single nucleotide repair or selective sequence modification of DNA. In a one-pot reaction, a single misincorporated ribonucleotide in a DNA strand was converted to the corresponding deoxyribonucleotide while maintaining sequence integrity. Furthermore, the sequences of DNA strands immobilized on multiple functional nanoparticles were successfully modified in order to control and alter the DNA-directed assembly of nanoparticles in a stepwise and selective fashion.

Results and discussion

To demonstrate that single nucleotide repair in DNA can be achieved by the cascade of two DNAzymes, we used a 26-nt DNA strand (**O1**) containing a misincorporated cytidine (rC) ribonucleotide as an example. The goal was to convert the rC in **O1** into a deoxycytidine (C), as seen in **O4** (Fig. 1a), while maintaining the integrity of the DNA sequence. The DNAzymes $17E_{m1}$ (Fig. 1a, blue) with RNA cleavage activity[2,57–59] and E47 (Fig. 1a, red) with DNA ligation activity[14,60] were chosen as the cascade pair in this study. The $17E_{m1}$ DNAzyme catalyzes the hydrolysis of the 3′ phosphodiester linkage of the internal rC in the DNA strand when metal ion cofactors such as Pb^{2+} and Zn^{2+} are present (Fig. S1a in ESI†). On the other hand, the E47 DNAzyme can induce the catalytic ligation of the 5′ –OH of the DNA substrate with another 3′-phosphorylated DNA strand (activated by imidazole)[14] in the presence of Cu^{2+} or Zn^{2+} as the metal cofactor (Fig. S1b in ESI†). Therefore, by sequential cleavage and ligation reactions catalyzed by these two DNAzymes on **O1** containing rC, **O1** could first be cleaved at the 3′ phosphodiester of the rC by $17E_{m1}$ and then undergo ligation at the cleavage site with another 3′-phosphorylated DNA strand of an identical sequence (except with deoxyribonucleotide C in place of ribonucleotide rC) by E47. The product **O4** has a sequence identical to the starting strand **O1**, with the rC replaced with C.

Initially, 3′-fluorescein-labeled **O1** was treated with $17E_{m1}$ to form DNA duplex **O1**-$17E_{m1}$ *via* 18 matched base pairs (9 on each binding arm). In the presence of Pb^{2+}, **O1** was efficiently cleaved by $17E_{m1}$ into fragments **O2** and **Oc**, resulting in the dehybridization of the duplex because the melting temperature of the duplex between $17E_{m1}$ and **O2** or between $17E_{m1}$ and **Oc** is below room temperature (Fig. 1a). The fluorescence image after polyacrylamide gel electrophoresis (PAGE) suggested the complete cleavage of **O1** and formation of **O2** (Fig. 2a, lane 1 and 2 for **O1** and **O2**, respectively), while **Oc** was not visible on the gel due to the lack of a fluorescein label. The cleavage reaction product **O2** was also confirmed by the result from matrix-assisted laser desorption ionization-time of flight (MALDI-TOF) mass spectrum (Table 1 and Fig. S2 in ESI†). Control experiments using a DNAzyme of a different sequence ($17E_{m2}$) or without Pb^{2+} showed negligible cleavage of the substrate **O1** (Fig. S3 in ESI†) due to the specificity of the DNAzyme and the essential role of the metal ion cofactor.[2,57–59] Subsequently, without any purification of **O2** from the mixture solution after the previous cleavage step, E47 and 3′-phosphorylated **O3** (imidazole-activated) were added into the solution to generate another DNA complex **O2**–**O3**-E47, which gave **O4** as the product after the E47-catalyzed ligation reaction in the presence of Cu^{2+} (Fig. 1a).[14,60] The formation of **O4** was confirmed by both fluorescent PAGE (Fig. 2a, the upper band of lane 3) and MALDI-TOF MS (Table 1 and Fig. S2 in ESI†), while some unreacted **O2** was also observed on the gel (Fig. 2a, the lower band of lane 3). Here, **O3** was invisible due to the lack of a fluorescein label. Considerably lower levels of ligation between **O2** and **O3** were observed if either E47 or Cu^{2+} was absent (Fig. S3 in ESI†). Together these results indicate that the reactions catalyzed by the DNAzyme cascade were achieved through a one-pot reaction without isolation and purification of the intermediate **O2**.

To provide further confirmation of the above successful conversion of rC in **O1** to C in **O4**, while keeping other sequences identical, a longer **O3 + 8A** (**O3** extended by A_8 at 5′) was used in place of **O3** (Fig. 1a). Under the same conditions, a longer product **O4 + 8A** was obtained (Fig. 2a, the upper band of lane 4) with slower gel migration compared to **O4** (Fig. 2a, the upper band of lane 3), suggesting that the ligation reaction occurred mostly between **O2** and imidazole-activated **O3**, and not between **O2** and un-activated **Oc** (**Oc** is the product from the previous cleavage reaction of **O1** and $17E_{m1}$), in which case a band with the same migration as **O4** would have been observed. The presence of C rather than rC in the product **O4** was supported by the lower molecular weight of **O4** in the MALDI-TOF mass spectrum as compared to that of **O1** (Table 1), as well as the increased resistance to hydrolysis of **O4** even in the presence of Pb^{2+} and $17E_{m1}$ (Fig. 2a, lane 5), which can catalyze the cleavage of a substrate containing an internal ribonucleotide linkage (**O1**),[2,57] but not a substrate containing entirely deoxyribonucleotides (**O4**).

In addition to the single nucleotide repair functionality, it is also possible to use this methodology to edit the sequence of a DNA strand, which was used to convert the DNA strand **O5** into **O4** using the same cascade and conditions as before (Fig. 1b and S4 in ESI†). The product **O4** was confirmed by PAGE (Fig. 2b) and MALDI-TOF MS (Table 1 and Fig. S2 in ESI†) and found to be identical to that obtained from the method in Fig. 1a.

Encouraged by the above results, we applied this method to modify the sequence of DNA immobilized on gold nanoparticles[27] (AuNPs) to control the DNA-directed assembly of the AuNPs in a selective manner. DNA-functionalized gold AuNPs have been used in a variety of applications due to both their

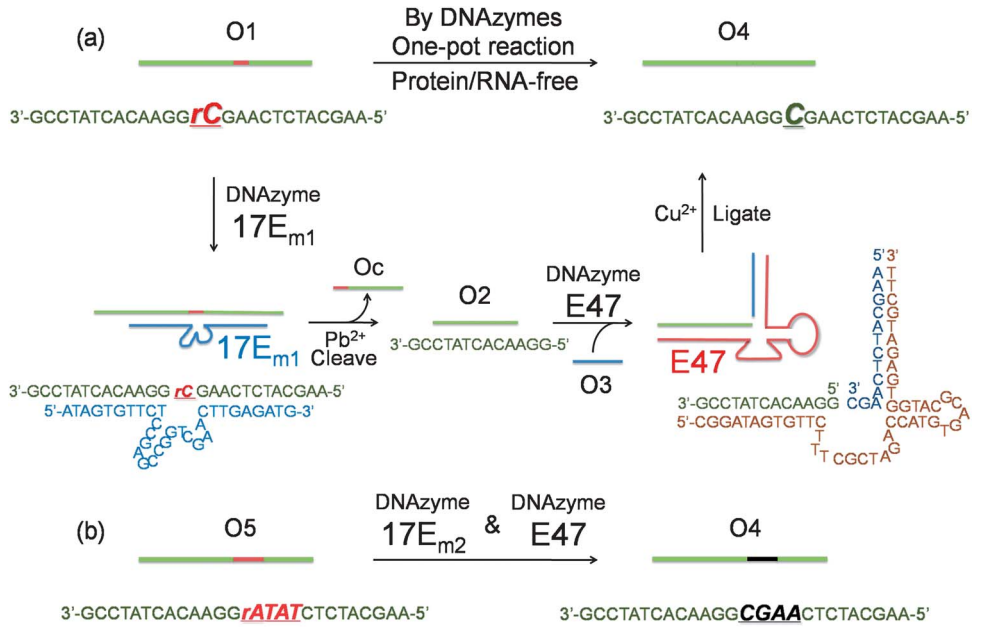

Fig. 1 (a) Conversion of a single ribonucleotide (rC) in a DNA strand **O1** to a deoxyribonucleotide (C) by the cascade of DNAzymes $17E_{m1}$ and E47: **O1** is cleaved by $17E_{m1}$ to afford products of **O2** and **Oc**; **O2** is then ligated with **O3** (activated by imidazole) to form **O4** by E47. (b) Sequence modification of a DNA strand **O5** to **O4** through a similar protocol by the cascade of DNAzymes $17E_{m2}$ and E47.

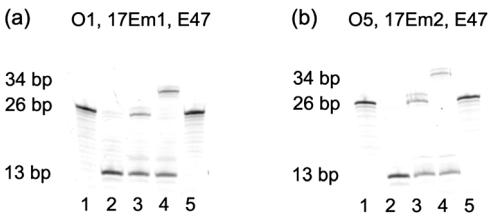

Fig. 2 (a) Fluorescent PAGE (20% denaturing gel) images of the transformation from **O1** to **O4** by DNAzymes $17E_{m1}$ and E47. Lanes in (a): **1**, **O1**; **2**, **1** after cleavage by $17E_{m1}$ to yield **O2** and **Oc** in the presence of Pb^{2+}; **3**, **2** after ligation to yield **O4** by E47 in the presence of **O3** and Cu^{2+}; **4**, **2** after ligation to yield **O4 + 8A** by E47 in the presence of **O3 + 8A** and Cu^{2+}; **5**, **O4** in the presence of Pb^{2+} and $17E_{m1}$. (b) Fluorescent PAGE images of the transformation from **O5** to **O4** by $17E_{m2}$ and E47: Lanes in (b): **1**, **O5**; **2**, **1** after cleavage by $17E_{m2}$ to yield **O2** in the presence of Pb^{2+}; **3**, **2** after ligation to yield **O4** by E47 in the presence of **O3** and Cu^{2+}; **4**, **2** after ligation to yield **O4 + 8A** by E47 in the presence of **O3 + 8A** and Cu^{2+}; **5**, **O4** in the presence of Pb^{2+} and $17E_{m2}$.

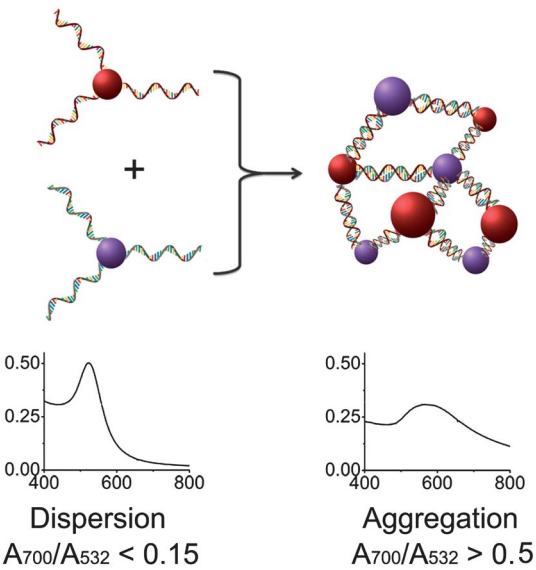

Fig. 3 Assembly of two types of DNA-functionalized gold nanoparticles. If the sequences of the two DNAs are not complementary, the gold nanoparticles are in a "dispersed" state and exhibit a red color with a sharp absorption band peaked around 532 nm (left). In contrast, the assembly of the gold nanoparticles with complementary DNAs causes the formation of an "aggregated" state with a broad absorption band around 600 nm (right).

Table 1 Measured and calculated molecular weight (*m*/*z*) in MALDI-TOF mass spectra of 3′-fluorescein-labeled DNAs (**O1**, **O2**, **O4** and **O5**). For full spectra, see Fig. S2 in ESI.†

DNA	O1	O2	O4	O5
Measured	8831.6	4824.1	8812.3	8819.1
Calculated	8831.9	4826.3	8815.9	8821.9

unique properties and the sequence-dependent hybridization of ssDNA immobilized on the AuNPs for controlled assembly.[51–55] As shown in Fig. 3, when AuNPs are functionalized by complementary DNAs, the AuNPs can assemble into an "aggregated" state *via* DNA hybridization, which shows red-shifted and broadened absorption spectra compared to AuNPs functionalized by non-complementary DNAs. By modifying the sequences of DNA on the AuNPs, the assembly of the particles can be effectively controlled. Although methods for fabrication of DNA-functionalized AuNPs have been developed,[27] there are still limited methods to modify the DNA sequences already

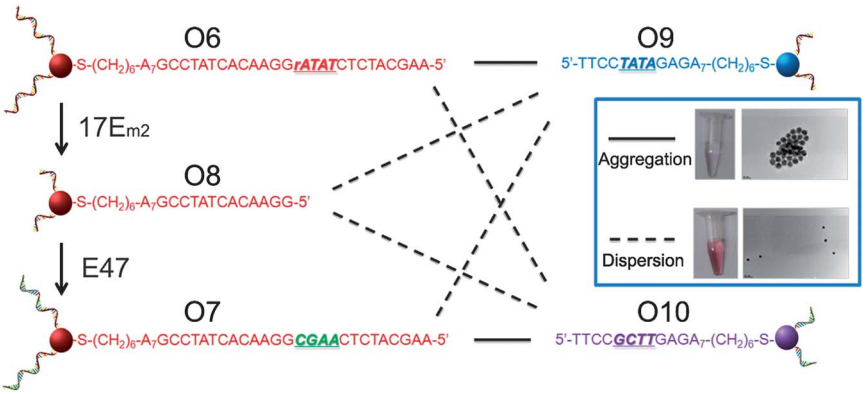

Fig. 4 Controlling the assembly of DNA-functionalized gold nanoparticles *via* cascade-mediated modification of the DNA sequences. The solid and dashed lines indicate the successful and unsuccessful formation of aggregates, respectively. The inset shows the assembly of AuNPs modified with the complementary strands **O6** and **O9** (top) and the lack of assembly between AuNPs modified with noncomplementary strands **O9** and **O7** (obtained by treating **O6**-functionalized AuNPs with $17E_{m2}$ and E47) (bottom).

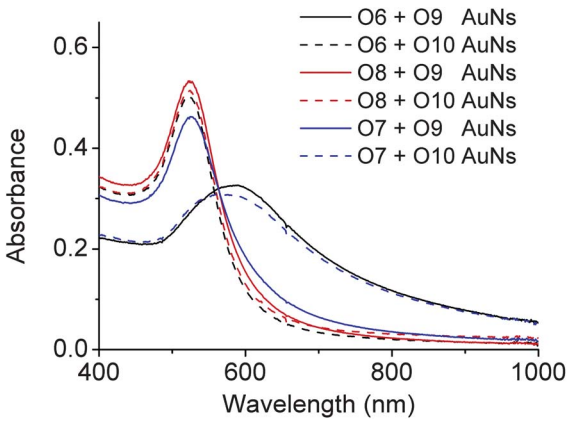

Fig. 5 Absorption spectra of **O6**-, **O7**- or **O8**-functionalized AuNPs in the presence of **O9**- and **O10**-functionalized AuNPs, respectively. The red-shift of the peak indicates the formation of AuNP aggregations due to the hybridization of complementary DNAs on the AuNPs.[27] For the ratios of absorbance (A_{700}/A_{532}), see Table S1 in ESI.†

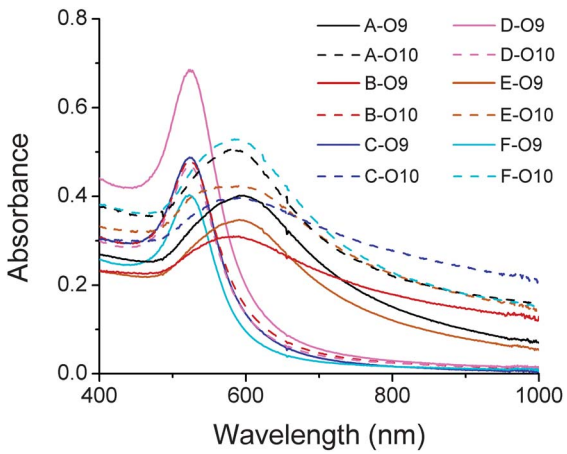

Fig. 7 Absorption spectra of DNA-functionalized gold nanoparticles (A–F) (Fig. 6a) in the presence of **O9**- and **O10**-functionalized AuNPs, respectively. The red-shift of the peak indicates the formation of AuNP aggregations due to the hybridization of complementary DNAs on the AuNPs.[27] For the ratios of absorbance (A_{700}/A_{532}), see Table S2 in ESI.†

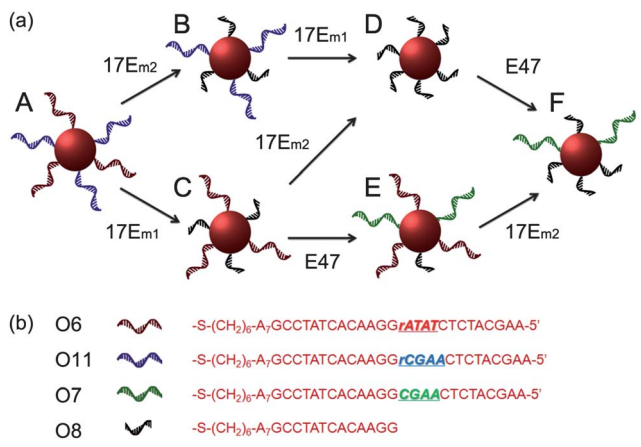

Fig. 6 (a) Scheme showing stepwise modification of DNA sequences on multiply-functional gold nanoparticles by the collaboration of $17E_{m1}$ or $17E_{m2}$ and E47. (b) DNA sequences of **O6–O8** and **O11**.

immobilized on AuNPs in order to tune their functions. It is even more challenging to modify a specific DNA sequence on multiply-functionalized AuNPs with different DNA sequences on each nanoparticle. Selective modification can allow each different function of the AuNP to be controlled in a selective fashion for potential applications.

AuNPs of 13 nm diameter were functionalized with DNA molecules *via* 3′-end thiols and used for this study. The formation of the AuNP assembly was confirmed by TEM images (Fig. S5 in ESI†) and characterized by large changes in absorption spectra[27] (A_{700}/A_{532} changed from <0.15 to >0.50 as illustrated in Fig. 5 and Table S1 in ESI†). As shown in Fig. 4, **O6**-functionalized AuNPs (red) were found to be able to form aggregates with **O9**-functionalized AuNPs (blue) *via* DNA-directed assembly through 12 complementary base pairs (Fig. 5 and S5 and Table S1†), but not with **O10**-functionalized AuNPs (purple), because of the 4 mismatched base pairs in the middle

of the binding arm (Fig. 5 and S5 and Table S1†). After being treated with $17E_{m2}$ and Pb^{2+}, the **O6** on the surface of AuNPs was cleaved and converted to **O8**, which could not hybridize with either **O9** or **O10** efficiently. Thus no DNA-directed assembly was observed between the resulting **O8**-functionalized AuNPs and either **O9**- or **O10**-functionalized AuNPs (Fig. 5 and S5 and Table S1†). However, after a subsequent ligation reaction catalyzed by E47 in the presence of imidazole-activated **O3** and Cu^{2+}, **O8** on the surface of AuNPs could be extended to **O7**, making the AuNPs capable of assembling with **O10**-, but not **O9**-functionalized AuNPs (Fig. 5 and S5 and Table S1†).

Interestingly, the product, **O7**-functionalized AuNPs, showed inverse characteristics in the formation of DNA-directed assembly with **O10**- and **O9**-functionalized AuNPs, compared to the original **O6**-functionalized AuNPs. TEM images of **O6**-functionalized AuNPs, either with or without treatment with $17E_{m2}$/E47, mixed with **O10**-functionalized AuNPs, are displayed in the inset of Fig. 4. These results clearly demonstrate that the ability to edit and replace DNA on AuNPs allows for exquisite programmable control over the assembly of nanoparticles.

Taking advantage of the specificity of DNAzyme to its nucleic acid substrates by complementary base pairing in the binding arms, selective modification of DNA sequences on surface of multiple functional AuNPs was also achieved in this work. As depicted in Fig. 6, **O6** (red) and **O11** (blue) bi-functional AuNPs could be modified by $17E_{m1}$, $17E_{m2}$ and E47 selectively and sequentially. As shown in Fig. 6, AuNPs capable of forming DNA-directed assembly with both (A and E), either (B, C and F), or neither (D) of the **O9**- and **O10**-functionalized AuNPs could be obtained by monitoring the significant increase of A_{700}/A_{532} as indication of assembly formation (Fig. 7 and Table S2 in ESI†). Such a result, which is challenging to achieve by other techniques, can be used for the construction of tunable nanoassemblies for various applications.

Conclusions

In summary, by putting together a cascade of two DNAzymes with cleaving and ligating activities, we have generated a new functionality for effective DNA modification. This function was applied in the conversion of a single misincorporated ribonucleotide into the corresponding dexoyribonucleotide in DNA and the modification of DNA sequences on the surface of gold nanoparticles to modify and control their self-assembly through DNA hybridization. The results suggest that combining DNAzymes with different catalytic activities may achieve more interesting functions and thus broaden the applications of DNAzymes.

Experimental section

Materials

All DNA samples were purchased from Integrated DNA Technologies Inc. (Coralville, IA). Substrate and enzyme strands of the DNAzyme were purified by HPLC; thiol-modified and phosphorylated DNAs underwent standard desalting. Other chemicals were purchased from Sigma-Aldrich Inc.

The sequences of DNA used in this work were as follows:

Cleaving DNAzyme $17E_{m1}$: 5′-ATAGTGTTCT CCGAGCCG GTCGAA **ATA**GAGATG-3′

Cleaving DNAzyme $17E_{m2}$: 5′-ATAGTGTTCT CCGAGCCG GTCGAA **CTT**GAGATG-3′

Ligating DNAzyme E47: 5′-CGGATAGTGTTCTTTCGCTAGAC CATGTGACGCATGG TGAGATGCTT-3′

Fluorescein-labeled substrate **O1**: 3′-**FAM**-GCCTATCACAAG G***rATAT***CTCTACGAA-5′

3′-phosphorylated **O3**: 3′-**PO_3**-CGAACTCTACGAA-5′

3′-phosphorylated **O3 + 8A**: 3′-**PO_3**-CGAACTCTACGAAAAAA AAAA-5′

Fluorescein-labeled substrate **O5**: 3′-**FAM**-GCCTATCACAAGG ***rCGAA***CTCTACGAA-5′

3′-thiol-modified **O6**: 3′-**HS**-AAAAAAAGCCTATCACAAGG***rAT AT***CTCTACGAA-5′

3′-thiol-modified **O9**: 3′-**HS**-AAAAAAAGAGATATCCTT-5′

3′-thiol-modified **O10**: 3′-**HS**-AAAAAAAGAGTTCGCCTT-5′

3′-thiol-modified **O11**: 3′-**HS**-AAAAAAAGCCTATCACAAGG***r C***GAA**CTCTACGAA-5′

Experimental procedures

DNAzyme ($17E_{M1}$ or $17E_{M2}$)-catalyzed cleavage of fluorescein-labelled substrate **O1** or **O5**. The 3′-fluorescein-labeled substrate DNA **O1** or **O5** (1 μM) was mixed with DNAzyme $17E_{m1}$ or $17E_{m2}$ (1 μM) and $Pb(NO_3)_2$ (5 μM) in 25 mM HEPES (pH 7.0) containing 100 mM NaCl. The mixture was incubated at room temperature for 1 h (for **O1**) or 3 h (for **O5**) to achieve complete cleavage (>95%) and subsequently analyzed by PAGE and MALDI-TOF MS.

Imidazole-activation of **O3** and **O3 + 8A**. In a 0.5 mL centrifuge tube, 20 μL 100 μM **O3** or **O3 + 8A** with 3′-phosphorylation were incubated with 2.5 μL of 1 M imidazole (pH 6.0, adjusted by adding concentrated HCl), and 4.5 μL of 1 M EDC·HCl at room temperature for 1 hour. The mixture was then purified with a PD-10 (Amersham Biosciences) desalting column, and the first fraction with strong absorption at 260 nm was collected (about 0.5–1.5 mL range). The DNA concentration of the eluted fraction was determined by monitoring the absorbance at 260 nm. The imidazole-activated **O3** and **O3 + 8A** were used right away, since they were not very stable at room temperature.

DNAzyme (E47)-catalyzed ligation of **O2**. The solution containing cleaved substrate from 17E treatment was further mixed with the ligation DNAzyme E47 (2 μM), $Cu(NO_3)_2$ (20 μM) and imidazole-activated **O3** or **O3 + 8A** (3 μM) in 25 mM HEPES (pH 7.0) containing 300 mM NaCl, and allowed to incubate at room temperature for 4 h before analysis by PAGE and MALDI-TOF MS.

PAGE and MALDI-TOF MS. 3′-fluorescein-labeled DNA samples (1 μM) were mixed in a 10 : 1 ratio with a stop solution containing 100 mM EDTA, to quench the cleavage and ligation reactions. This solution was mixed 1 : 1 with glycerol and transferred to a denaturing 20% acrylamide gel. The resulting gel was documented by a fluorescence image scanner (model

FLA-3000G, Fuji). DNA isolation from the gel was performed by soaking the cut-out gel band in 1 mL Millipore water for 1 day, then centrifuging at 10 000 rpm for 15 minutes. Afterwards, the fluorescent supernatant was concentrated to about 20 μL and purified by PD-10 column. The fraction with fluorescence at 520 nm was collected (total volume approximately 0.5–1.5 mL), concentrated to 20 μL, and then analyzed by MALDI-TOF MS.

Nanoparticle preparation and functionalization (**O6**, **O9**, **O10** and **O11**). The preparation of 13 nm gold nanoparticles was as reported.[27] DNAs with 3′-thiol-modifications (**O6**, **O9**, **O10** and **O11**) were activated by incubation with TCEP. Typically, 9 μL of 1 mM DNA in Millipore water was incubated with 1 μL of 20 mM freshly prepared TCEP and 1 μL 500 mM NaAc–HAc buffer (pH 5.2) at room temperature for 1 hour. The mixture was then directly added into 3 mL of citrate-capped 13 nm AuNPs (about 3 nM). After incubation for 16 hours at room temperature, 0.3 mL of buffer containing 1 M NaCl and 100 mM of tris-acetate (pH 8.2) was added by drop to the nanoparticle solution under stir. After incubation for 24 hours, the nanoparticles were centrifuged at 13 000 rpm for 15 minutes. The supernatant was removed and nanoparticles were re-dispersed in buffer containing 100 mM NaCl and 25 mM tris-acetate (pH 8.2). This centrifugation process was repeated once more to remove free DNA in solution.

For nanoparticles functionalized with both **O6** and **O11** in sequential tuning experiments, the molar ratio of **O6** and **O11** in loading was 4 : 1, with a total loading amount of 25 μL of 1 mM DNA. Other procedures were the same as above.

DNAzyme ($17E_{m1}$ or $17E_{m2}$)-catalyzed cleavage of DNA on gold nanoparticles (**O6** and **O11**). DNA-functionalized gold nanoparticles were centrifuged at 13 000 rpm for 15 minutes. The supernatant was removed and nanoparticles were re-dispersed in a buffer containing 100 mM NaCl and 25 mM HEPES (pH 7.0) to prepare a 3 nM solution. Then DNAzyme $17E_{m1}$ or $17E_{m2}$ (3 μM) and $Pb(NO_3)_2$ (4 μM) were added to the solution. The mixture was incubated at room temperature for 10 hours, then centrifuged at 13 000 rpm for 15 minutes. The supernatant was removed and nanoparticles were re-dispersed in 1 mM HEPES (pH 7.0) without NaCl for 15 min to denature DNA hybridization. This centrifugation process was repeated once to remove free DNA in solution. At last, gold nanoparticles were re-dispersed in 100 mM NaCl and 25 mM HEPES (pH 7.0) to prepare a 3 nM solution.

DNAzyme (E47)-catalyzed ligation of DNA on gold nanoparticles (**O8**). The above solution was mixed with E47 (3 μM), $Cu(NO_3)_2$ (20 μM) and imidazole-activated **O3** (4 μM) in 25 mM HEPES (pH 7.0) containing 150 mM NaCl. Then the mixture was incubated at room temperature for 16 hours. After that, nanoparticles were centrifuged at 13 000 rpm for 15 minutes. The supernatant was removed and nanoparticles were re-dispersed in 1 mM HEPES (pH 7.0) without NaCl for 15 min to denature DNA hybridization. This centrifugation process was repeated twice to remove free DNA in solution. Finally, the nanoparticles were re-dispersed in 100 mM NaCl and 25 mM HEPES (pH 7.0) to a final concentration of 3 nM.

Formation of gold nanoparticle assemblies. DNA-functionalized gold nanoparticles were washed and re-dispersed in 100 mM NaCl and 25 mM HEPES (pH 7.0) to prepare 3 nM solutions as mentioned above. Equal volumes of **O6**-, **O7**- or **O8**-functionalized AuNPs (3 nM), **O9**- or **O10**-functionalized gold nanoparticles (3 nM), and 1 M NaCl were mixed. After vortexing, the resulting solution was incubated at room temperature for at least 1 hour to form nanoparticle assemblies.

TEM. Gold nanoparticles were analyzed using a JEOL 2010LaB6 transmission electron microscope (TEM) operated at 200 kV. Samples were prepared by putting a drop of nanoparticle solutions onto a carbon-coated copper TEM grid (Ted Pella).

Acknowledgements

We wish to thank the US National Institute of Health (ES016865) and Department of Energy (DE-FG02-08ER64568) for financial support.

Notes and references

1 D. L. Robertson and G. F. Joyce, *Nature*, 1990, **344**, 467–468.
2 R. R. Breaker and G. F. Joyce, *Chem. Biol.*, 1994, **1**, 223–229.
3 D. Sen and C. R. Geyer, *Curr. Opin. Chem. Biol.*, 1998, **2**, 680–687.
4 Y. F. Li and R. R. Breaker, *Curr. Opin. Struct. Biol.*, 1999, **9**, 315–323.
5 Y. Lu, *Chem.–Eur. J.*, 2002, **8**, 4588–4596.
6 R. R. Breaker, *Nature*, 2004, **432**, 838–845.
7 K. Schlosser and Y. F. Li, *Chem. Biol.*, 2009, **16**, 311–322.
8 S. K. Silverman, *Acc. Chem. Res.*, 2009, **42**, 1521–1531.
9 R. R. Breaker and G. F. Joyce, *Chem. Biol.*, 1995, **2**, 655–660.
10 N. Carmi, S. R. Balkhi and R. R. Breaker, *Proc. Natl. Acad. Sci. U. S. A.*, 1998, **95**, 2233–2237.
11 A. R. Feldman and D. Sen, *J. Mol. Biol.*, 2001, **313**, 283–294.
12 J. W. Liu, A. K. Brown, X. L. Meng, D. M. Cropek, J. D. Istok, D. B. Watson and Y. Lu, *Proc. Natl. Acad. Sci. U. S. A.*, 2007, **104**, 2056–2061.
13 M. Chandra, A. Sachdeva and S. K. Silverman, *Nat. Chem. Biol.*, 2009, **5**, 718–720.
14 B. Cuenoud and J. W. Szostak, *Nature*, 1995, **375**, 611–614.
15 A. Sreedhara, Y. F. Li and R. R. Breaker, *J. Am. Chem. Soc.*, 2004, **126**, 3454–3460.
16 W. E. Purtha, R. L. Coppins, M. K. Smalley and S. K. Silverman, *J. Am. Chem. Soc.*, 2005, **127**, 13124–13125.
17 Y. F. Li and R. R. Breaker, *Proc. Natl. Acad. Sci. U. S. A.*, 1999, **96**, 2746–2751.
18 Y. F. Li, Y. Liu and R. R. Breaker, *Biochemistry*, 2000, **39**, 3106–3114.
19 T. L. Sheppard, P. Ordoukhanian and G. F. Joyce, *Proc. Natl. Acad. Sci. U. S. A.*, 2000, **97**, 7802–7807.
20 Y. F. Li and D. Sen, *Nat. Struct. Biol.*, 1996, **3**, 743–747.
21 D. Sen and L. C. H. Poon, *Crit. Rev. Biochem. Mol. Biol.*, 2011, **46**, 478–492.
22 M. Chandra and S. K. Silverman, *J. Am. Chem. Soc.*, 2008, **130**, 2936–2937.

23 P. I. Pradeepkumar, C. Hobartner, D. A. Baum and S. K. Silverman, *Angew. Chem., Int. Ed.*, 2008, **47**, 1753–1757.
24 P. Travascio, Y. F. Li and D. Sen, *Chem. Biol.*, 1998, **5**, 505–517.
25 L. C. H. Poon, S. P. Methot, W. Morabi-Pazooki, F. Pio, A. J. Bennet and D. Sen, *J. Am. Chem. Soc.*, 2011, **133**, 1877–1884.
26 D. J. F. Chinnapen and D. Sen, *Proc. Natl. Acad. Sci. U. S. A.*, 2004, **101**, 65–69.
27 C. A. Mirkin, R. L. Letsinger, R. C. Mucic and J. J. Storhoff, *Nature*, 1996, **382**, 607–609.
28 J. W. Liu and Y. Lu, *J. Am. Chem. Soc.*, 2003, **125**, 6642–6643.
29 Y. Li and Y. Lu, *Functional Nucleic Acids for Sensingand Other Analytical Applications*, Springer, New York, 2009.
30 J. W. Liu, Z. H. Cao and Y. Lu, *Chem. Rev.*, 2009, **109**, 1948–1998.
31 M. M. Ali, S. D. Aguirre, H. Lazim and Y. F. Li, *Angew. Chem., Int. Ed.*, 2011, **50**, 3751–3754.
32 I. Willner, B. Shlyahovsky, M. Zayats and B. Willner, *Chem. Soc. Rev.*, 2008, **37**, 1153–1165.
33 Y. Chen, M. S. Wang and C. D. Mao, *Angew. Chem., Int. Ed.*, 2004, **43**, 3554–3557.
34 A. Peracchi, *Rev. Med. Virol.*, 2004, **14**, 47–64.
35 A. M. Pyle, V. T. Chu, E. Jankowsky and H. Boudvillain, *Methods Enzymol.*, 2000, **317**, 140–146.
36 M. Isildar, M. N. Schuchmann, D. Schultefrohlinde and C. Vonsonntag, *Int. J. Radiat. Biol.*, 1981, **40**, 347–354.
37 P. S. Eder, R. Y. Walder and J. A. Walder, *Biochimie*, 1993, **75**, 123–126.
38 N. C. Horton and B. C. Finzel, *J. Mol. Biol.*, 1996, **264**, 521–533.
39 S. Nakano, T. Kanzaki and N. Sugimoto, *J. Am. Chem. Soc.*, 2004, **126**, 1088–1095.
40 C. M. Joyce, *Proc. Natl. Acad. Sci. U. S. A.*, 1997, **94**, 1619–1622.
41 K. J. Scanlon, M. Kashanisabet and H. Miyachi, *Cancer Invest.*, 1989, **7**, 581–587.
42 B. Rydberg and J. Game, *Proc. Natl. Acad. Sci. U. S. A.*, 2002, **99**, 16654–16659.
43 N. Kim, S. Y. N. Huang, J. S. Williams, Y. C. Li, A. B. Clark, J. E. Cho, T. A. Kunkel, Y. Pommier and S. Jinks-Robertson, *Science*, 2011, **332**, 1561–1564.
44 S. J. Park, T. A. Taton and C. A. Mirkin, *Science*, 2002, **295**, 1503–1506.
45 N. L. Rosi and C. A. Mirkin, *Chem. Rev.*, 2005, **105**, 1547–1562.
46 C. S. Thaxton, D. G. Georganopoulou and C. A. Mirkin, *Clin. Chim. Acta*, 2006, **363**, 120–126.
47 Z. D. Wang and Y. Lu, *J. Mater. Chem.*, 2009, **19**, 1788–1798.
48 H. Wang, R. H. Yang, L. Yang and W. H. Tan, *ACS Nano*, 2009, **3**, 2451–2460.
49 W. Xu, X. J. Xue, T. H. Li, H. Q. Zeng and X. G. Liu, *Angew. Chem., Int. Ed.*, 2009, **48**, 6849–6852.
50 F. Wang, Y. Han, C. S. Lim, Y. H. Lu, J. Wang, J. Xu, H. Y. Chen, C. Zhang, M. H. Hong and X. G. Liu, *Nature*, 2010, **463**, 1061–1065.
51 S. Y. Park, A. K. R. Lytton-Jean, B. Lee, S. Weigand, G. C. Schatz and C. A. Mirkin, *Nature*, 2008, **451**, 553–556.
52 J. Sharma, R. Chhabra, A. Cheng, J. Brownell, Y. Liu and H. Yan, *Science*, 2009, **323**, 112–116.
53 Y. Wang, G. Chen, M. X. Yang, G. Silber, S. X. Xing, L. H. Tan, F. Wang, Y. H. Feng, X. G. Liu, S. Z. Li and H. Y. Chen, *Nat. Commun.*, 2010, DOI: 10.1038/ncomms1089.
54 A. V. Pinheiro, D. R. Han, W. M. Shih and H. Yan, *Nat. Nanotechnol.*, 2011, **6**, 763–772.
55 Z. Zhao, E. L. Jacovetty, Y. Liu and H. Yan, *Angew. Chem., Int. Ed.*, 2011, **50**, 2041–2044.
56 W. A. Zhao, J. C. F. Lam, W. Chiuman, M. A. Brook and Y. F. Li, *Small*, 2008, **4**, 810–816.
57 J. Li and Y. Lu, *J. Am. Chem. Soc.*, 2000, **122**, 10466–10467.
58 Y. Okumoto, Y. Tanabe and N. Sugimoto, *Biochemistry*, 2003, **42**, 2158–2165.
59 S. Nakano, H. T. Karimata, Y. Kitagawa and N. Sugimoto, *J. Am. Chem. Soc.*, 2009, **131**, 16881–16888.
60 J. W. Liu and Y. Lu, *Chem. Commun.*, 2007, 4872–4874.